Imaging Subcortical Auditory Activity in Humans

A.R. Guimaraes,[1,2*] **J.R. Melcher,**[3] **T.M. Talavage,**[2,3] **J.R. Baker,**[1,2] **P. Ledden,**[1]
B.R. Rosen,[1,2] **N.Y.S. Kiang,**[2–4] **B.C. Fullerton,**[2,3] **and R.M. Weisskoff**[1,2]

[1]*MGH-NMR Center, Department of Radiology, Massachusetts General Hospital,
Charlestown, Massachusetts 02129*
[2]*Harvard-Massachusetts Institute of Technology Division of Health, Sciences and Technology,
Cambridge, Massachusetts 02139*
[3]*Eaton-Peabody Laboratory, Massachusetts Eye and Ear Infirmary, Boston, Massachusetts*
[4]*Department of Brain and Cognitive Sciences, Massachusetts Institute of Technology,
Cambridge, Massachusetts 02139*

◆ ─────────────────────────────── ◆

Abstract: There is a lack of physiological data pertaining to how listening humans process auditory information. Functional magnetic resonance imaging (fMRI) has provided some data for the auditory cortex in awake humans, but there is still a paucity of comparable data for subcortical auditory areas where the early stages of processing take place, as amply demonstrated by single-unit studies in animals. It is unclear why fMRI has been unsuccessful in imaging auditory brain-stem activity, but one problem may be cardiac-related, pulsatile brain-stem motion. To examine this, a method eliminating such motion (using cardiac gating) was applied to map sound-related activity in the auditory cortices and inferior colliculi in the brain stem. Activation in both the colliculi and cortex became more discernible when gating was used. In contrast with the cortex, the improvement in the colliculi resulted from a reduction in signal variability, rather than from an increase in percent signal change. This reduction is consistent with the hypothesis that motion or pulsatile flow is a major factor in brain-stem imaging. The way now seems clear to studying activity throughout the human auditory pathway in listening humans. *Hum. Brain Mapping 6:33–41, 1998.* © **1998 Wiley-Liss, Inc.**

◆ ─────────────────────────────── ◆

INTRODUCTION

Much of the detailed information about physiological activity in the auditory nervous system is derived from animal studies using invasive techniques [Irvine, 1992; Phillips et al., 1991]. Direct neurophysiological data from humans are considerably less detailed [Lauter et al., 1995; Pantev et al., 1988; Picton et al., 1974; Romani et al., 1982], although the psychophysical capabilities for hearing are probably better documented for humans than for any other species [Long, 1994; Moore, 1989]. Recently, blood-oxygenation level-dependent functional magnetic resonance imaging (fMRI) has emerged as a noninvasive method for spatially mapping activity in the brain [Bandettini et al., 1992; Kwong et al., 1992]. A number of imaging studies on humans have described sound-evoked cortical activity [Binder et al., 1994; Talavage et al., 1996; Wessinger et al., 1995], but no studies have reported activity for the brain-stem auditory regions where most of the auditory neurophysiological data in anesthetized or restrained animals have been gathered.

Other noninvasive methods such as evoked potential measurement, magnetoencephalography, and positron emission tomography each have their own limitations in assaying brain-stem function. Auditory-

evoked potentials can provide information about particular brain-stem cell populations [Melcher and Kiang, 1996]; magnetoencephalographic signals from brain-stem structures approach the limits of detectability [Erné and Hoke, 1990]; images of specific subcortical auditory structures have not thus far been demonstrated with positron emission tomography. If brain-stem auditory activity could be measured with fMRI, a new way to study subcortical auditory processing in behaving humans would be available, and human psychophysical data could be related to animal neurophysiological data more readily.

It is not clear why brain-stem activity (demonstrable in electrophysiological recordings [Hashimoto et al., 1981; Møller and Jannetta, 1983; Starr and Hamilton, 1976]) has not been readily imaged with fMRI. The difficulties may be due to unfavorable anatomical characteristics of the vascular system, the nature of the neuronal activity, or the fact that the brain stem moves with each arterial pulsation, as is often seen when the brain stem is surgically exposed [Britt and Rossi, 1982; Poncelet et al., 1992].

Here we demonstrate a novel variation on standard fMRI technique that eliminates any confounding effects of pulsatile brain-stem motion. In a standard fMRI paradigm, magnetic resonance (MR) images are acquired while stimuli are repeatedly turned on and off. The MR signal-changes that are temporally correlated with the stimulus presentations are considered "activity" [Bandettini et al., 1992; Kwong et al., 1992]. Using such standard paradigms, we can demonstrate auditory activity routinely in the cortex, but only rarely in the brain stem. Two modifications were therefore made: 1) image acquisitions were synchronized to a particular time in the subject's cardiac cycle ("cardiac gating" [Vlaardingerbroek and den Boer, 1996]), and 2) a postacquisition correction was applied to adjust for interimage variations in signal intensity caused by fluctuations in heart rate. Here, we demonstrate that images of auditory activity in the brain stem are improved using this approach.

SUBJECTS AND METHODS

Data were obtained from 8 volunteers (4 male and 4 female) using a 1.5 T scanner (General Electric) retrofitted for echo-planar imaging (by Advanced NMR Systems, Inc.). The volunteers gave informed consent for participation in this study. They were then placed supine in the scanner and imaged using a head coil. The subject's head was immobilized by a custom-molded bite-bar mounted on the head coil. For each subject, 1) Contiguous sagittal images of the whole head were acquired, and used to select the slice for functional imaging. The imaging plane was chosen to cut through the transverse temporal gyri of the cortex and the inferior colliculi in the brain stem, so that all four auditory stations could be monitored simultaneously (Fig. 1). This plane sometimes also intersects parts of the medial geniculate bodies in the thalamus [De Armond et al., 1976; Talairach and Tournoux, 1988]. 2) Echoplanar-based shimming was performed [Reese et al., 1995]. 3) A T1-weighted, high-resolution image was acquired of the brain slice to be functionally imaged (TR = 4,000 msec; TI = 1,300 msec; TE = 75 msec; in-plane resolution = 1.5×1.5 mm). 4) Functional imaging was performed while the subject listened to an acoustic stimulus presented in a standard "on/off" paradigm. Specifically, magnetic resonance images (asymmetric spin echo, TE = 70 msec, τ offset = 25 msec, thickness = 7 mm) were acquired every 2 sec ("ungated"). In order to preserve approximately the same repetition rate, the "gated" images were acquired every other heartbeat, because the normal heart rate varies between 60–80 beats per min, which translates into a repetition rate of 660 msec–1 sec/beat. In the gated condition, the subject's electrocardiogram was measured and used to trigger the scanner. The acoustic stimulus was orchestral music, chosen because it routinely produces robust activation in the transverse temporal gyri. For each functional image, the music was turned on for 30 sec and off for 30 sec for a total of four repetitions. The same musical segment was presented during each music "on" epoch (first 30 sec of the fourth movement in Beethoven Symphony No. 7 in A Major, played at a comfortable listening level).

The music was delivered binaurally through a headphone assembly that also attenuated the ambient noise and imager-generated sounds. Specifically, the music was played by a compact disc player which drove a pair of acoustic transducers housed in a shielded box adjacent to the scanner. The sound output of the transducers was conveyed to the subject's ears via air-filled tubes. Earmuffs designed for ear protection in noisy industrial environments were placed over the ears. These muffs were fitted with a coupler linking the tube from the transducer to the air cavity under the muff at the subject's ear.

Postacquisition image processing

Since heart rate typically fluctuates, the interimage time with cardiac gating also fluctuates from image to image. This variability in interimage time translates directly into signal intensity changes because of the
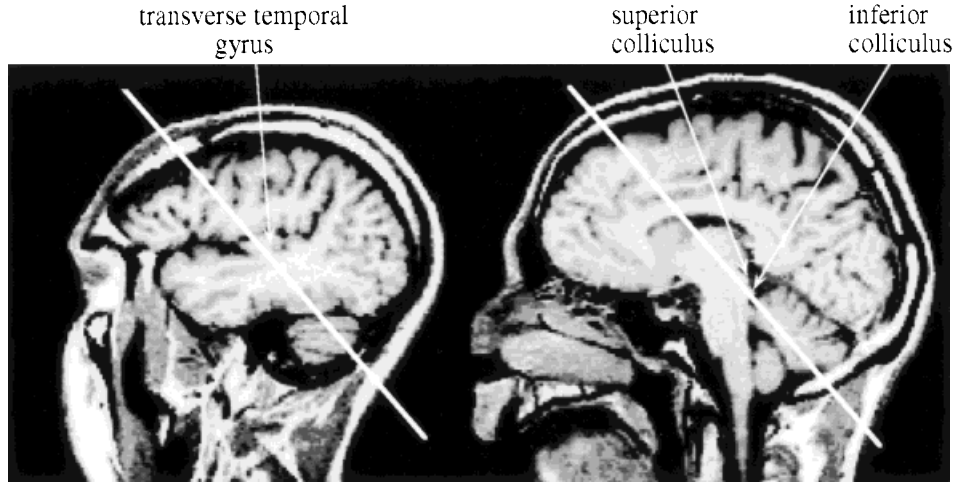
Figure 1.
Subject 1. Functional imaging plane superimposed on two sagittal, anatomical images. The functional plane (thick white lines) passed through the inferior colliculi and the transverse temporal gyri.

exponential relationship between the residual longitudinal magnetization and interimage time. These signal intensity changes compromised the statistical confidence of functional images by increasing the variance and were therefore corrected using an algorithm that required measuring the interval of time that elapsed between consecutive images. The correction assumes that image signal strength is proportional to the exponential recovery in longitudinal magnetization between successive image acquisitions. Then,

$$S_{i,n} = A_{i,n}[1 - \exp(-t_n/T1_i)] \qquad (1)$$

where $S_{i,n}$ is the measured signal for the ith voxel and the nth acquisition, t_n is the time between the $n - 1$ and nth acquisitions, $T1_i$ is the effective longitudinal relaxation time for the ith voxel, and $A_{i,n}$ would be the maximum signal amplitude for the ith voxel at the nth acquisition without the T1-weighting. The t_n were measured using a computer interfaced to the scanner; the scanner produced a trigger pulse each time an image was acquired, and the computer recorded the time between successive triggers. Inverting Equation (1) as the definition of $A_{i,n}$ (i.e., $A_{i,n} = S_{i,n} [1 - \exp(-t_n/T1_i)]^{-1}$), $T1_i$ were estimated by minimizing the variance of the $A_{i,n}$ time series:

$$MSE = (1/N) \sum_{n=1}^{N} [A_{i,n} - (1/N) \sum_{m=1}^{N} A_{i,m}]^2 \qquad (2)$$

where N is the total number of acquisitions. Signals were then corrected to the value they would have had if the interval between acquisitions had been constant and equal to the average interacquisition interval T_{av}. Thus, the corrected signal

$$S_{i,n}' = A_{i,n}[1 - \exp(-T_{av}/T1_i)] \qquad (3)$$

where $T_{av} = (1/N) \sum_{n=1}^{N} t_n$.

"Ungated" images and corrected "gated" images were processed identically to generate activation maps. First, a standard algorithm (statistical parametric mapping) was applied to the images to correct for in-plane subject motion. Then, regions of activation were defined using Student's unpaired t-test to compare image signal strength and variability during music "on" and music "off" periods. The resulting activation maps (in-plane resolution 3.1×3.1 mm) were interpolated to have the same resolution (1.5×1.5 mm) as the anatomical images obtained during the same experimental session. The activation maps and anatomical images were then superimposed.

Anatomical identification of auditory structures

So that activation could be studied on a region-by-region basis, the limits of each auditory structure in our imaging plane were determined. The border of the inferior colliculus was defined as the perimeter of a circle fit (by eye) to the posterior convexity of the colliculus, which was easily identified in the anatomical images (e.g., see Fig. 2). The superior temporal plane included all of the temporal lobe superior to the superior temporal sulcus. Standard anatomical atlases
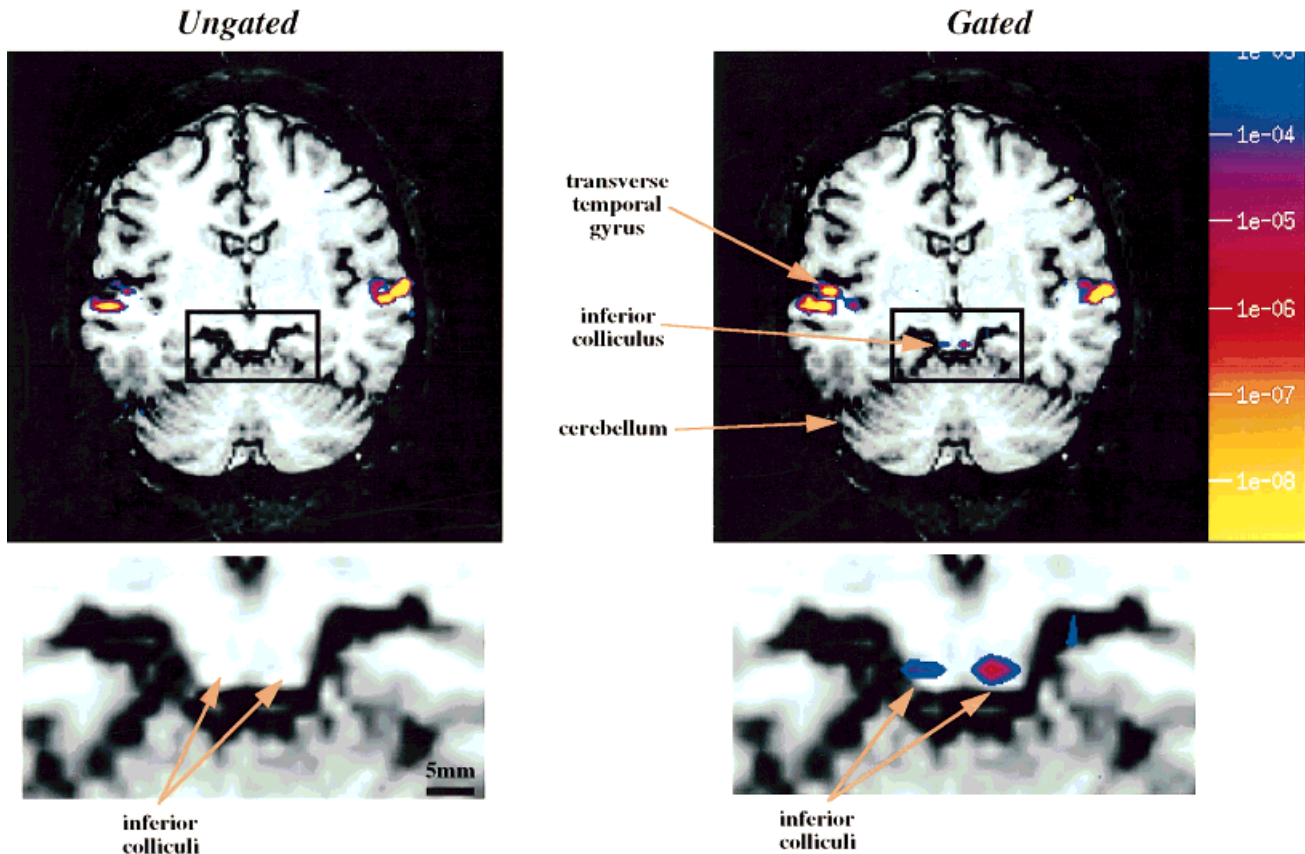
Figure 2.

Subject 1. fMRI activation maps in response to music without (**left**) and with (**right**) gating and correction. For both conditions, the same slice passing through the transverse temporal gyri and inferior colliculi was imaged while music was repeatedly turned on for 30 sec and off for 30 sec. Regions are colored according to (approximate) *P*-value based on Student's unpaired t-test on MR signal differences between music "on" and music "off" periods. Blue and yellow correspond to the lowest ($P = 0.001$) and highest ($P = 2 \times 10^{-9}$) levels, respectively. The activation maps (which are based on functional images with an in-plane resolution of 3.1×3.1 mm) have been interpolated and superimposed on T1-weighted, high-resolution anatomical images acquired during the same imaging session. The rectangles (top) enclosing the inferior colliculi indicate the area of the enlargements seen at the bottom. Activation maps for the ungated and the gated cases are based on 270 and 324 images, respectively, representing 9 min of data in both cases.

[De Armond et al., 1976; Talairach and Tournoux, 1988] were used to delimit a region enclosing the medial geniculate body (MGB), since the MGB was not directly identifiable in the anatomical images. Areas of activation ($P < 0.005$) were attributed to the MGB when they overlapped this anatomically defined "MGB region." The anterior edge of the ambient cistern was used to define the posterior extent of the MGB region. The distance from the region's posterior edge to its anterior edge was determined from measurements of the anteroposterior extent of the MGB in the atlases. The distances between the midline and the medial and lateral edges of the MGB region were determined by measuring the distances between the midline and the medial and lateral edges of the MGB in the atlases, normalizing the atlas measurements to maximum brain width, and multiplying the normalized atlas measurements by the maximum width of the individual imaged brain slice.

RESULTS

Figure 2 shows the results using both the ungated and the gated paradigms. The top two images show clear bilateral activity in and lateral to the transverse

temporal gyri (auditory cortical areas [Galaburda and Sanides, 1980; Rademacher et al., 1993]). The two lower images are enlargements of the boxed regions in the top images and include the inferior colliculi, which are easily identified as prominent "bumps" immediately anterior to the cerebellum. The ungated image shows far less activity in the colliculi (t-score = 2.92 (right colliculus), 2.47 (left)) than does the gated image (t-score = 4.24 (right), 5.65 (left)). The activated volume in each colliculus corresponds to roughly one voxel in the original functional images.

In each inferior colliculus in each subject, the voxel with the highest t-score was identified separately in gated and ungated activation maps. Out of the 16 colliculi in our 8 subjects, 14 showed higher t-scores with gating as compared with no gating ($P < 0.01$, sign test for paired observations). Averaged across colliculi, the t-score with gating (3.55 ± 1.14; mean $\pm$ standard deviation) was significantly greater than without gating (2.43 ± 0.97; $P < 0.01$, Wilcoxon signed rank test). Thus, on balance, our ability to detect collicular activation was clearly improved by using the gating paradigm.

Since t-scores depend on both signal variability and the difference in signal level between stimulus "on" and "off" periods, either or both of these factors could account for the improvements in brain-stem activation with gating. To understand the relative importance of these factors, image signals in the inferior colliculus were examined more closely. These analyses focused on a region of interest defined for each subject by 1) delimiting the inferior colliculi in the high-resolution anatomical image, and 2) using the activation maps to identify the region (volume = 32 μl) in each colliculus with the highest t-score. The latter step was performed separately using the ungated and gated activation maps. Three quantities were calculated for each region of interest: 1) the percent change in signal intensity between the music "on" and the music "off" periods, 2) the standard deviation in signal intensity during the music "on" periods, and 3) the standard deviation during the music "off" periods. The values for these quantities in the gated condition were then compared with those in the ungated condition. Comparisons were made using Student's two-tailed paired t-test (percent signal change) or the Wilcoxon signed rank test (standard deviation). As summarized in Table I, there was a statistically significant ($P < 0.01$) decrease in standard deviation with gating, but no significant difference in percent signal change. Thus, the decrease in standard deviation accounts for the increase in collicular activation with gating. The decrease in stan-

dard deviation was comparable during the music "on" and music "off" conditions, indicating that the activation itself did not contribute substantially to signal variability. For comparison, signal levels in the cortex were also analyzed using methods identical to those for the collicular analyses, except that the region of interest (volume = 896 μl) consisted of the highest t-score regions on the two superior temporal planes. There was an increase in percent signal change with gating and no significant difference in standard deviation (Table I), so there was also an increase in cortical activation with gating.

Although our experiments were designed to investigate the inferior colliculus and auditory cortex, our imaging plane sometimes intersected with the medial geniculate body in the thalamus. Analysis of the data demonstrated that 6 out of 8 subjects in the "gated" condition and 5 out of 8 subjects in the "ungated" condition showed a focus of activation immediately adjacent to the lateral extreme of the ambient cistern (Fig. 3A, B) where the medial geniculate body is located. The localization of medial geniculate body activation can be verified by comparing the anatomical images and superimposed activation maps in Figure 3A, B with the computerized human brain atlas in Figure 3C, which shows the spatial relationship between the medial geniculate body, ambient cistern, and inferior colliculus in the imaged plane.

DISCUSSION

By demonstrating that subcortical auditory structures can be imaged readily with fMRI when the effects of cardiac-related brain motion are taken into account, we have identified an important technical variable to control in imaging studies of the brain stem. Cardiac gating eliminates the effect of motion that is directly correlated to the cardiac rhythm by acquiring images at the same time postsystole within the cardiac cycle. The fact that reductions in signal variability were seen with gating in the inferior colliculus, but not the cortex, is consistent with the interpretation that there is greater absolute movement of the colliculus than of the cortex over the course of the cardiac cycle. The data demonstrate that gating with correction increases the time series signal-to-noise ratio within the colliculus by decreasing the variance within these regions, and by decreasing it comparably in both the "rest" and "active" states. The lack of an increase in percent signal change within this same region implies that rhythmic variation in partial voluming of the collicular activation is not responsible for its difficulty in being de-

TABLE I. Region of interest analysis comparing percent signal change and standard deviation between gated and ungated conditions within the inferior colliculus and auditory cortex*

	Percent signal change	Standard deviation, music on	Standard deviation, music off
Inferior colliculus			
Ungated	0.80 ± 0.23	20.5 ± 5.7	19.9 ± 5.0
Gated	0.80 ± 0.32	13.9 ± 1.5	14.2 ± 1.5
	NS	$P < 0.01$	$P < 0.01$
Auditory cortex			
Ungated	1.50 ± 0.45	13.8 ± 0.8	13.9 ± 0.7
Gated	2.10 ± 0.52	13.9 ± 0.8	14.6 ± 1.0
	$P < 0.01$	NS	NS

*Signal change and signal variability with and without gating in regions of interest within the inferior colliculus and auditory cortex. For each subject, a collicular region of interest was identified by 1) determining the border around each inferior colliculus (as described in Subjects and Methods), and 2) identifying the highest t-score region (volume of 32 μl) in each colliculus in interpolated activation maps (in-plane resolution 1.5×1.5 mm, voxel volume 16 μl). The "high t-score" regions in the two colliculi together defined the collicular region of interest. Percent signal change, standard deviation during the music "on" periods, and standard deviation during the "off" periods were calculated for each voxel in a region of interest, and were then averaged across voxels. The mean and standard deviation are given for each quantity. Average values based on "gated" data were compared with those based on "ungated" data using Student's two-tailed paired t-test (percent signal change) or the Wilcoxon signed rank test (standard deviation). Analyses for the auditory cortex were the same except that the region of interest consisted of the highest t-score regions on the superior temporal planes. The volume for this cortical region of interest (896 μl total, 448 μl on each superior temporal plane) was chosen to be comparable to that of the collicular region of interest as follows. First, the volume with $P < 0.01$ on the superior temporal planes and in the inferior colliculi was determined for each subject based on the gated activation maps. The volume for the collicular region of interest was 40% of the "$P < 0.01$ volume" in the colliculi (average across subjects = 160 μl), so that the cortical region of interest was 40% of the "$P < 0.01$ volume" (2,250 μl) on the superior temporal planes. NS, not significant.

tected in the ungated studies. However, it is possible that imaging even smaller structures (i.e., subvoxel) could reveal improvements in both percent signal change and time-series variance.

The gating method we used is extendable to multiple imaging planes, thereby increasing the number of structures that can be simultaneously studied. Increases in sensitivity may also be achievable by combining our procedures with other technical modifications such as using higher field strengths or reducing the scanner-produced background acoustic noise. These or other methods [Hu et al., 1995] that attempt to correct

for physiological fluctuations should be applicable to studies of lower brain-stem structures of comparable size to the colliculus, such as the cochlear nucleus or the superior olivary complex [Kiang et al., 1984; Moore, 1987; Winer, 1984]. Even with current capabilities it may be possible to resolve subnuclei within classically defined auditory structures (e.g., the dorsal vs. ventral cochlear nucleus or the dorsal vs. ventral divisions of the medial geniculate body).

An interesting point is that all of the clearly responding regions in our imaged plane were localizable to classically-defined auditory projection nuclei. Having shown that activity can be detected in these nuclei, one may well ask why our present experimental paradigm does not demonstrate activation in other areas that are also known to contain neurons that respond to sound. It is well-established that electrophysiological responses to acoustic stimuli are recordable from single units in such regions as the reticular formation and the deep layers of the superior colliculi [Allon and Wollberg, 1978; Jones, 1975; King and Palmer, 1983; Middlebrooks and Knudsen, 1984; Rouiller et al., 1985; Villa, 1990], regions typically sampled in our imaging plane [De Armond et al., 1976; Talairach and Tournoux, 1988] (Figs. 1–3). It may be that activation in these regions was "washed out" by partial volume effects, and might be detectable using smaller voxels. It may also be that acoustically-evoked neuronal activity in these regions is too low in level or concentration to generate a significant response in functional images. This could, for example, account for the lack of clear activation in the superior colliculi, since single units in this region have low discharge rates in response to acoustic stimulation, even in lightly or unanesthetized animals [Allon and Wollberg, 1978; King and Palmer, 1983; Middlebrooks and Knudsen, 1984]. Perhaps maintaining detailed information about an acoustic stimulus (e.g., in the inferior colliculus) requires much more neuronal activity than is needed to encode stimulus location (e.g., in the superior colliculus). It may also be that auditory information can be conveyed in changing temporal patterns of activity without necessarily changing the overall level of activity. Clearly, the relative responsiveness of different subcortical areas to auditory stimulation has fundamental implications for stimulus coding, and is therefore an important direction for future, more systematic exploration.

The method introduced here offers opportunities for studying information processing in humans throughout the auditory pathway. More specifically, it should now be possible to examine the respective roles of cortical and subcortical structures in processing sound
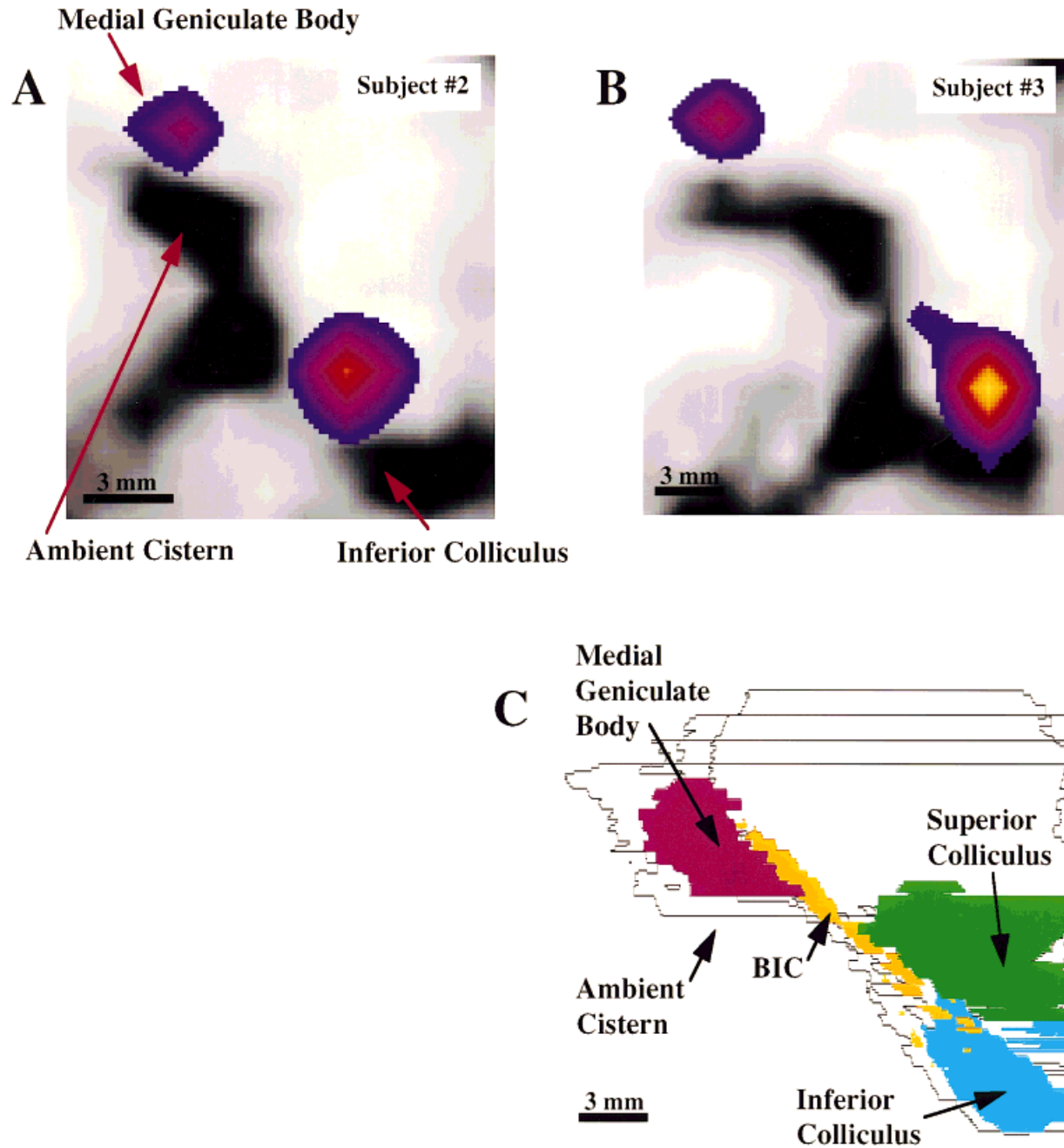
Figure 3.
A, B: Activation maps superimposed on anatomical images in 2 subjects with activity in the medial geniculate body. Region shown is comparable to the left half of the enlargements in Figure 2. In the activation maps, blue and yellow correspond to the lowest ($P = 0.01$) and highest ($P = 2 \times 10^{-9}$) significance levels, respectively. **C:** Four slices through a computerized atlas of a human brain. The slices (80-μm-thick, separated by 1,600 μm) were angled to correspond to the imaging plane in A and B, and were positioned at four evenly-spaced locations through the thickness (7 mm) of the imaged slice. The colored areas show the maximum in-plane extent of each structure. The atlas was created from postmortem, histologically-prepared, serially-sectioned human brain tissue [Kiang et al., 1984]. The medial geniculate body, superior colliculus, and inferior colliculus were delimited based on standard cytoarchitectonic criteria. The brachium of the inferior colliculus (BIC) includes axons projecting between the colliculus and the medial geniculate body.

stimuli under various listening conditions, for different subject states, and during the performance of well-defined psychophysical tasks. It should also be possible to investigate the role that subcortical auditory structures might play in communication disorders known or speculated to have auditory components, including tinnitus [Møller, 1995; Shulman, 1991], autism [Litrownik and McInnis, 1982], and dyslexia [Tallal et al., 1993]. Obviously, our methods can be adopted for other systems in the brain stem and may be useful in studying other species.

ACKNOWLEDGMENTS

REFERENCES

Allon N, Wollberg Z (1978): Responses of cells in the superior colliculus of the squirrel monkey to auditory stimuli. Brain Res 159:321–330.

Bandettini PA, Wong EC, Hinks RS, Rikofsky RS, Hyde JS (1992): Time course EPI of human brain function during task activation. Magn Reson Med 25:390–397.

Binder JR, Rao SM, Hammeke TA, Yetkin FZ, Jesmanowicz A, Bandettini PA, Wong EC, Estkowski LD, Goldstein MD, Haughton VM (1994): Functional magnetic resonance imaging of human auditory cortex. Ann Neurol 35:662–672.

Britt RH, Rossi GT (1982): Quantitative analysis of methods for reducing physiological brain pulsations. J Neurosci Methods 6:219–229.

De Armond SJ, Fusco MM, Dewey MM (1976): Structure of the Human Brain, 2nd ed. New York: Oxford University Press.

Erné SN, Hoke M (1990): Short-latency evoked magnetic fields from the human auditory brainstem. Adv Neurol 54:167–176.

Galaburda A, Sanides FJ (1980): Cytoarchitectonic organization of the human auditory cortex. J Comp Neurol 190:597–610.

Hashimoto I, Ishiyama Y, Yoshimoto T, Nemoto S (1981): Brain-stem auditory-evoked potentials recorded directly from human brain-stem and thalamus. Brain 104:841–859.

Hu X, Le TH, Parrish T, Erhard P (1995): Retrospective estimation and correction of physiological fluctuation in functional MRI. Magn Reson Med 34:201–212.

Irvine DRF (1992): Physiology of the auditory brainstem. In: Popper A, Fay R (eds): The Mammalian Auditory Pathway: Neurophysiology. New York: Springer-Verlag, pp 153–231.

Jones EG (1975): Some aspects of the organization of the thalamic reticular complex. J Comp Neurol 162:285–308.

Kiang NYS, Fullerton BC, Richter EA, Levine RA, Norris BE (1984): Artificial stimulation of the auditory system. Adv Audiol 1:6–17.

King AJ, Palmer AR (1983): Cells responsive to free-field auditory stimuli in guinea-pig superior colliculus: Distribution and response properties. J Physiol 342:361–381.

Kwong KK, Belliveau JW, Chesler DA, Goldberg IE, Weisskoff RM, Poncelet BP, Kennedy DN, Hoppel BE, Cohen MS, Turner R,

Cheng HM, Brady TJ, Rosen BR (1992): Dynamic magnetic resonance imaging of human brain activity during primary sensory stimulation. Proc Natl Acad Sci USA 89:5675–5679.

Lauter JL, Herscovitch P, Formby C, Raichle ME (1995): Tonotopic organization in human auditory cortex revealed by positron emission tomography. Hear Res 20:199–205.

Litrownik AJ, McInnis ET (1982): Cognitive and perceptual deficits in autistic children: A model of information processing, critical review, and suggestions for the future. In: Steffen JJ, Karoly P (eds): Autism and Severe Psychopathology. Toronto: D.C. Heath and Company, pp 103–155.

Long GR (1994): Psychoacoustics. In: Fay RR, Popper AN (eds): Comparative Hearing: Mammals. New York: Springer-Verlag, pp 18–56.

Melcher JR, Kiang NYS (1996): Generators of the brainstem auditory evoked potential in cat III: Identified cell populations. Hear Res 93:52–71.

Middlebrooks JC, Knudsen EI (1984): A neural code for auditory space in the cat's superior colliculus. J Neurosci 4:2621–2634.

Møller AR (1995): Pathophysiology of tinnitus. In: Vernon JA, Møller AR (eds): Mechanisms of Tinnitus. Boston: Allyn and Bacon, pp 207–217.

Møller AR, Jannetta PJJ (1983): Auditory evoked potentials recorded from the cochlear nucleus and its vicinity in man. J Neurosurg 59:1013–1018.

Moore BCJ (1989): An Introduction to the Psychology of Hearing, New York: Academic Press.

Moore JK (1987): The human auditory brain stem: A comparitive view. Hear Res 29:1–32.

Pantev C, Hoke M, Lehnertz K, Lutkenhoner B, Anogianakis G, Wittkowski W (1988): Tonotopic organization of the human auditory cortex revealed by transient auditory evoked magnetic fields. Electroencephalogr Clin Neurophysiol 69:160–170.

Phillips DP, Reale RA, Brugge JF (1991): Stimulus processing in the auditory cortex. In: Altshuler RA, Bobbin RP, Clapton BM, Hoffman DW (eds): Neurobiology of Hearing: The Central Auditory System. New York: Raven Press, pp 335–365.

Picton TW, Hillyard SA, Krausz HI, Galambos R (1974): Human auditory evoked potentials. I: Evaluation of components. Electroencephalogr Clin Neurophysiol 36:191–199.

Poncelet BP, Wedeen VJ, Weisskoff RM, Cohen MS (1992): Brain parenchyma motion: Measurement with cine echo-planar MR imaging. Radiology 185:645–651.

Rademacher J, Caviness VS, Steinmetz H, Galaburda AM (1993): Topographical variation of the human primary cortices: Implications for neuroimaging, brain mapping, and neurobiology. Cereb Cortex 3:313–329.

Reese TG, Davis TL, Weisskoff RM (1995): Automated at 1.5T using echo-planar image frequency maps. J Magn Reson Imag 5:739–745.

Romani GL, Williamson SJ, Kaufman L (1982): Tonotopic organization of the human auditory cortex. Science 216:1339–1340.

Rouiller EM, Colomb E, Capt M, de Ribaupierre F (1985): Projections of the reticular complex of the thalamus onto physiologically characterized regions of the medial geniculate body. Neurosci Lett 53:227–232.

Shulman A (1991): Tinnitus models: A basis for the evaluation of the pathophysiology of tinnitus. In: Shulman A, Aran JM, Feldman H, Tonndorf J, Vernon JA (eds): Tinnitus. Philadelphia: Lea and Febiger, pp 67–98.

Starr A, Hamilton AE (1976): Correlation between confirmed sites of neurological lesions and abnormalities of far-field auditory

brainstem responses. Electroencephalogr Clin Neurophysiol 41: 595–608.

Talairach J, Tournoux P (1988): Co-Planar Stereotaxic Atlas of the Human Brain. New York: Thieme Medical Publishers.

Talavage TT, Ledden PJ, Sereno MI, Benson RR, Rosen BR (1996): Preliminary [fMRI] evidence of tonotopic organization in human auditory cortex. Neuroimage 3:355.

Tallal P, Miller S, Fitch RH (1993): Neurobiological basis of speech: A case for the preeminence of temporal processing. Ann NY Acad Sci 27–47.

Villa AEP (1990): Physiological differentiation within the auditory part of the thalamic reticular nucleus of the cat. Brain Res Rev 15:25–40.

Vlaardingerbroek MT, den Boer JA (1996): Magnetic Resonance Imaging, New York: Springer-Verlag.

Wessinger CM, Buonocore M, Kussmaul CL, Mangun GR, Jones A, Gazzaniga MS (1995): Functional magnetic resonance imaging of auditory cortex using pulsed tones. Soc Neurosci Abstr 694.

Winer JA (1984): The human medial geniculate body. Hear Res 15:225–247.